Fuel 228 (2018) 429–437

Contents lists available at ScienceDirect

Fuel

journal homepage: www.elsevier.com/locate/fuel

Full Length Article

Molecular characterization of kerogen and its implications for determining hydrocarbon potential, organic matter sources and thermal maturity in Marcellus Shale

Vikas Agrawal*, Shikha Sharma

Department of Geology and Geography, West Virginia University, Morgantown, WV, United States

ARTICLE INFO

Keywords:
Kerogen
Organic matter
Thermal maturity
Marcellus Shale
NMR

ABSTRACT

Organic-rich shales are a vital component of the US energy sector. Kerogen, a high molecular weight macromolecule is the largest reservoir of organic carbon on earth and serves as the starting material for the oil and gas generation in these shales. Despite its importance, kerogen structure and its evolution on maturation are still not well understood, especially for mature shales (VRo > 1). Moreover, most of the models built to determine hydrocarbon (HC) potential and thermal maturity of the source rocks have used the structural parameters of kerogen extracted from immature shales (VRo < 1). Therefore, these models might not yield accurate results for mature and over-mature shales like Marcellus. In this study, we determine the structural parameters of kerogen extracted from three Marcellus Shale cores using ^{13}C solid-state Nuclear magnetic resonance (NMR). Samples were acquired from the upper and lower Marcellus Shale Formation from a dry gas well WV-6 (VRo > 2.5), a wet gas well WV-7 (VRo ~ 1.4) and an oil window well BG-1 (VRo ~ 0.81) in Monongalia, Wetzel and Brooke County, West Virginia, respectively. Our results indicate that the percentage of carbon chains such as mobile (freely rotating) and immobile alkyl without heteroatoms (with restricted rotation), and alkyl-substituted aromatic carbons decrease with increasing maturity indicating that these chains are more prone to thermal degradation and might have higher HC generating potential. However, carbon chains such as O- substituted alkyl (ether), O_2 substituted alkyl (dioxy alkyl), amine, protonated aromatic carbons, O- substituted aromatic (phenol) and bridgehead aromatic carbons does not decrease directly with thermal maturity suggesting that these groups are either more refractory in nature or their carbon fraction is influenced by changing sources of OM. Our results also indicate that the previous models based on the structural parameters of kerogen derived from immature shales overestimate the HC generation potential and underestimate the thermal maturity in mature shales from the Marcellus. In addition, H, O, C ratios derived from structural parameters of kerogen can be utilized to determine the kerogen type in these mature shales where traditional pyrolysis analysis fails to characterize the kerogen.

1. Introduction

Kerogen, the insoluble fraction oforganic matter (OM) in sedimentary rocks, is the largest and economically most important reservoir of organic carbon and source of all hydrocarbons in the subsurface. Therefore, it is essential to accurately characterize the structure of kerogen and its HC generation potential. However, there is a significant gap in understanding the mechanism of kerogen cracking and HC generation especially for mature shales (VRo > 1) mostly due to the insolubility and chemical heterogeneity of kerogen. Additionally, limited analytical techniques have the ability to provide quantitative molecular-level information of the structure of kerogen [7,16,48].

Kerogen is formed by the degradation, condensation, and polymerization of biomolecules contributed by different sources of OM (e.g., [21,45,18,48]. Kerogen formed in the diagenetic stage of burial later cracks to form oil and gas in catagenetic and metagenetic stages of burial. Most of the current studies on kerogen have been focused on methods such as visual kerogen analysis and pyrolysis using a Source Rock Analyzer (SRA). These methods are helpful in determining the type of kerogen, maturity, and oil vs. gas generating potential but do not provide any information on the chemical structure or composition of kerogen [48]. Moreover, for mature/over-mature source rocks SRA produces biased results about the OM sources and maturity due to low amounts of free/bound hydrocarbons, and incomplete combustion of

* Corresponding author at: Department of Geology and Geography, West Virginia University, 330 Brooks Hall, 98 Beechurst Ave., Morgantown, WV 26506, United States.
E-mail address: viagrawall@mix.wvu.edu (V. Agrawal).

https://doi.org/10.1016/j.fuel.2018.04.053
Received 14 December 2017; Received in revised form 9 April 2018; Accepted 10 April 2018

refractory OM, and/or the hydrocarbons bound in a mineral matrix [48]. Biomarker ratios have also been used to determine the thermal maturity of source rocks [40,24,3,26]. However, due to thermal degradation and alteration of biomarkers on maturation and low extraction efficiency in high maturity samples, the results can be biased.

To understand kerogen cracking mechanism at the molecular level and to accurately predict HC potential from any source rock, it is vital to understand the molecular structure of kerogen [5,47,48]. Several analytical techniques have been developed for characterization of the chemical structure of kerogen, which are commonly classified into two major groups: destructive (pyrolytic) and non-destructive (spectroscopic) methods [46,8,9]. The pyrolytic analyses can provide valuable information about the labile/pyrolyzable fraction of kerogen [5,20,42,29]. However, the products generated from pyrolysis can interact among themselves and yield biased results about the components present in the labile fraction of kerogen [20]. Moreover, most of the kerogen models developed using the yield from pyrolysis experiments are conducted under elevated temperature (~250–650 °C) and then extrapolated to ~100 to 170 °C [17,49]. These results may not be reliable as the time span differs by ~4 orders of magnitude [17,49]. Additionally, the pyrolysis results depend on whether the reaction is conducted in an open vs. closed or hydrous vs. anhydrous conditions [6,28]. Therefore, the reactions taking place in laboratory conditions might not be representative of sedimentary basin conditions. Due to these limitations, non-destructive methods such as Fourier transform infrared (FT-IR), Raman spectroscopy (RS), X-ray photoelectron spectroscopy (XPS), X-ray diffraction (XRD), and ^{13}C solid-state nuclear magnetic resonance (^{13}C NMR) have been employed for the qualitative, semi-quantitative, and quantitative measurements of kerogen [13,52,25,41,46].

The ^{13}C solid-state NMR techniques provide the maximum amount of structural information on kerogen due to its higher accuracy and quantification capacity compared to other direct analytical methods, [33]. The most extensively used solid-state NMR technique for kerogen characterization is ^{13}C cross polarization/magic angle spinning (CP/MAS) [13,52,39,32,29,50]; [25]; [51,31,30]. However, by using ^{13}C CP/MAS alone, the fraction of non-protonated carbons and mobile groups (with non-restricted rotation) cannot be determined. Therefore, advanced solid-state NMR techniques such as multiple CP /MAS, multiple CP /MAS plus dipolar dephasing have been developed and applied in the recent years for systematically characterizing kerogen [33,23]. These advanced ^{13}C NMR techniques can be used for determining specific functional groups, aromaticity, and aromatic cluster size and better understanding the chemical structure of kerogen. A few researchers have used advanced NMR techniques, to determine the molecular structure of kerogen (For, e.g. [25,46,31,30]. However, most of these studies were conducted mainly on low maturity or immature samples. The models developed using these immature shales [27,31,50] can result in underestimation/overestimation of HC potential (especially gas) and thermal maturity, especially in mature shales with VRo > 1. For accurate estimation of HC potential in newly emerging mature shale plays like Marcellus, there is a need to develop a better understanding of the molecular structure of kerogen in mature shales with VRo > .1

The goal of the study is to determine changes in structural parameters of kerogen using ^{13}C solid-state NMR in Marcellus Shale maturity series with VRo ranging from 0.8 to 2.5. Kerogen was extracted from sediments from upper and lower Marcellus Shale Formation from three wells lying in the oil window (BG-1), wet gas window (WV-7) and in the dry gas window (WV-6). The location of the three wells is shown in Fig. 1. The easternmost WV-6 core has a thermal maturity of VRo > 2.5, WV-7 core has VRo ~ 1.4 [1,53], and the BG-1 core has VRo ~ 0.81–1.05. The depositional environment of the wells WV-6 and WV-7 has been established using geochemical, isotopic, pyrolysis and biomarker proxies [12,1]. The depositional model proposed by these studies suggest that the terrestrial sediment influx was from east to west

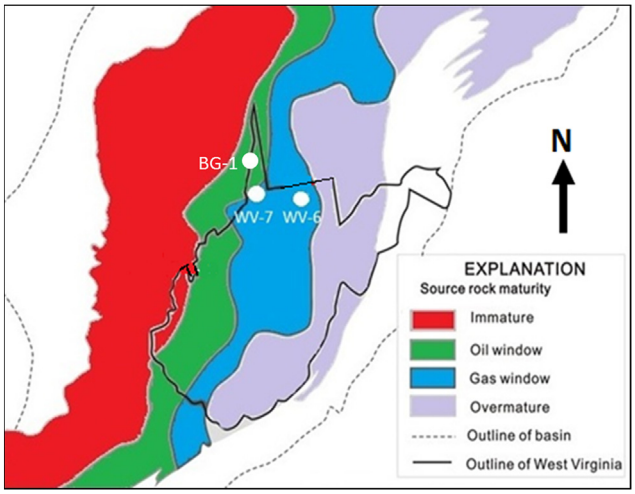

Fig. 1. Location of wells BG-1, WV-7 and WV-6. Modified from [54].

part of the basin, and the model suggests that sediments in dry gas WV-6 well were deposited in shallower part of the basin and received higher terrestrial OM influx as compared to WV-7 shale that was deposited in the deeper and anoxic part of the basin. Further, it was shown that upper Marcellus Formation received more terrestrial OM input as compared to lower Marcellus Shale Formation. Detailed isotopic and geochemical study is not available for the well BG-1. However, since this well is located in the western part of the basin (Fig. 1), the sediments must have been deposited further away from the terrestrial sediment source.

2. Materials and methods

2.1. Sampling

Core samples have been collected from three wells (WV-6, WV-7, and BG-1) in the upper and lower zones of the Marcellus Shale Formation. Location of WV-6 is in Monongalia County, WV-7 is from Wetzel County, and BG-1 is from Brooke County, West Virginia. (as shown in Fig. 1). To avoid any effects of contamination due to contact with drilling fluids and oxidation of OM [37,15] at least 5 mm of the outer layer of samples was removed before kerogen extraction. It is highly unlikely for fluids or air to penetrate > 5 mm of shale layer and contaminate/oxidize the inner part of the core. After paring, the inner portion was crushed to 200 mesh and homogenized using a sterile SPEX mixer mill and oven dried for 24 h at 50 °C.

2.2. Kerogen extraction

Kerogen was extracted from shale cores using methods modified from previous studies [14,48,22]. Soluble OM was extracted by sonicating 50 g of powdered samples in approximately 120 ml of dichloromethane DCM multiple times till the color of the solution was transparent. The residue was sonicated again with ~20 ml MeOH–acetone–$CHCl_3$ (15:15:70 v/v) mixture to dissolve the remaining polar soluble OM. The carbonates mineral was then dissolved from the residue by adding 6 N HCl for 48–72 h. This step was done multiple times until no effervescence was observed. Silicate minerals and the carbonates bound in silicate minerals were dissolved using a 1:1 mixture of 6 N HCl and 50% HF for 24 h. The residue was thoroughly rinsed with distilled water to avoid the formation of fluoride minerals. Remaining silicate minerals were dissolved by using 50% HF multiple times. Each HF step was followed by multiple rinses with distilled water to avoid neo-fluoride formation. Heavy minerals such as pyrite were removed by separating the denser phase by using 2.4gm/cc zinc bromide. The

lighter phase containing the kerogen was decanted. The extracted residue was sonicated again with DCM to remove the soluble OM which was bound in mineral matrix and kerogen. Kerogen extraction was done at IsoBioGem Lab at Department of Geology and Geography, West Virginia University, Morgantown.

2.3. ^{13}C solid-state NMR analysis

Solid-state NMR measurements were performed at Environmental NMR Service at Old Dominion University in Norfolk, Virginia, USA on a Bruker Advance III 400 spectrometer operating at 400-MHz 1H and 100-MHz ^{13}C frequencies. The ^{13}C chemical shifts were referenced to tetramethylsilane, using the COO resonance of glycine in the α-modification at 176.46 ppm as a secondary reference. The high-spinning speed multi-ramped amplitude cross polarization/magic angle spinning technique developed by [23] was applied for acquiring quantitative ^{13}C NMR spectra for all the kerogen samples. This multiple-cross polarization (multiCP) technique provides a simple but a powerful tool to obtain quantitative ^{13}C NMR spectra of organic materials, with high signal-to-noise ratio. The spectra were measured at a spinning speed of 14 kHz, where spinning sidebands are fairly small (< 3%) and had little overlap with center bands. To differentiate nonprotonated C from total C and to determine fractions of mobile groups (with no restricted rotation), ^{13}C multiCP/MAS with dipolar dephasing was performed under the same conditions as for 13C multiCP/MAS but combined with a dipolar dephasing time of 68 μs [35]. The relative proportion of different carbon chains such as mobile and immobile alkyl without heteroatoms (written just as alkyl in this study), methoxy and amine, O-substituted and O_2 substituted alkyls (ethers and dioxy alkyl), protonated aromatic, bridgehead aromatic, alkyl substituted aromatic, O- substituted aromatic (phenol), carboxyl, carbonyl were obtained for ^{13}C NMR spectrum using an NMR peak fitting program *TopSpin* (as shown in Fig. 2, area of spectra from 0 to 240 ppm was considered to be 100%). Error associated with NMR analysis is reported as ± Standard deviation (Table 1). Standard deviation is calculated as: Integral of area of interest × 1/SINO, where SINO is signal to noise ratio. Noise to signal ratio for the total region (from 0 to 240 ppm) was generally < 2%.

3. Results & discussion

3.1. Structural parameters of kerogen

Different aliphatic and aromatic carbon chains have characteristic chemical shifts in an NMR spectra as shown in Table 1 [44,27,4,43]. Dipolar dephasing method with multiple CP method allows the quantification of mobile aliphatic and protonated (and non-protonated) aromatic carbon chains along with other aliphatic and aromatic chains as shown in Table 1 [36,33,34,35,8]. The aliphatic and the aromatic fraction in the NMR spectra lies in 0–90 ppm and 90–165 ppm chemical shift range respectively. The fractions of different aliphatic and aromatic chains in kerogen extracted from upper and lower Marcellus of BG-1, WV-6, and WV-7 shale cores were calculated using the peak area of the respective chemical shifts in an NMR spectrum (Table 1, Fig. 2). The fractions of aliphatic carbon, alkyl (without heteroatoms), methoxy and amine, O and O_2 substituted alkyl carbons (ether and dioxy alkyl), total aromatic carbon, alkyl substituted aromatic, O-substituted aromatic (phenol), carboxyl and amide, aldehyde and ketone were determined using the multiple CP method (without dipolar dephasing). However, the fractions of mobile (freely rotating) and immobile (restricted rotation) methyl, mobile and quaternary alkyl (without heteroatoms), methoxy, protonated aromatic, non-protonated aromatic bridgehead carbon (fa^B) were determined using dipolar dephasing method with multiple CP (Table 1, Fig. 2). Using these aliphatic and aromatic structural parameters, several lattice structural parameters such as fraction of aromatic carbons with attachments or substituents (FAA), average aliphatic carbon chain length (Cn'), average carbons per aromatic cluster (C) and SP^2/SP^3 hybridized carbon ratio was determined [19,25] to construct kerogen models (Table 1 of Supplementary Information). FAA was determined by dividing the sum of alkyl substituted aromatic carbon fraction and phenolic carbon fraction with the total aromatic fraction. Cn' was determined by dividing the fraction of aliphatic carbon with the alkyl substituted aromatic fraction. Average carbons per aromatic cluster (C) was determined by the equation proposed by Solum et al., 2001. SP^2/SP^3 hybridized carbon was determined by dividing the peak area 90–240 ppm to 0–90 ppm in multiple CP NMR spectra.

The peak area distribution using ^{13}C multiple CP NMR spectra shows that BG-1 kerogen samples have the highest average percentage of aliphatic carbon chains (28%) followed by WV-7 (26%) and WV-6 (~14%) (Fig. 3a). In all the six kerogen samples, the majority of aliphatic chains are alkyl chains with no heteroatoms (Fig. 3a). Alkyl carbon chains (without heteroatoms) followed a trend similar to total aliphatic carbon. The BG-1 kerogen samples had the highest average fraction of these carbon chains (23%) followed by WV-7 kerogen samples (~22%) and WV-6 kerogen samples (9%). However, O and O_2 substituted alkyl carbon does not follow a simple trend with increasing maturity, it decreases from BG-1 (~3.5%) to WV-7 (~2.2%) kerogen samples and then increases in WV-6 kerogen (~4.1%). It was also observed that BG-1 upper Marcellus (~30% aliphatic and 26% alkyl) had relatively higher total aliphatic and alkyl fraction than lower Marcellus (25% aliphatic and 20% alkyl) kerogen sample but the total aliphatic and alkyl fraction in lower and upper Marcellus was similar for both WV-6 and WV-7 wells (Fig. 3a) within the same well. On the contrary, O and O_2 substitute alkyl groups were significantly different for upper and lower Marcellus kerogen for all the three wells (Fig. 3a).

Peak area distribution shows a lowest fraction of aromatic carbon in kerogen samples from BG-1 (67–70%) followed by WV-7 (73–75%) and WV-6 (85–89%) (Fig. 3b). A similar trend was observed for protonated aromatic carbon and bridgehead aromatic carbon, but an opposite trend was observed for alkyl substituted aromatic carbon (Table 1, Fig. 3b). The percentage fraction of O-substituted aromatic carbons decreases from BG-1 to WV-7 kerogen, but increases on further maturation from WV-7 to WV-6, similar to the trend observed for O and O_2 substituted aliphatic carbon chains. Comparison of the upper and lower Marcellus kerogen sample in individual wells shows that in BG-1 well, upper Marcellus Formation had relatively higher protonated aromatic carbon fraction and lower total aromatic and bridgehead fraction compared to lower Marcellus Formation (Fig. 3b). However, in wells WV-6 and WV-7, samples from both upper and lower Marcellus Formation had similar fractions of total aromatic, protonated, aromatic bridgehead and alkyl substituted aromatic carbon chains within the individual well (Fig. 3b).

Lattice structural parameters FAA shows a general decrease in average number of carbon per aromatic cluster (C) and a general increase in SP^2/SP^3 hybridized carbon ratio from BG-1 to WV-7 to WV-6 (Fig. 3c, Table 1 in Supplementary Information). However, Cn' increases from BG-1 (1.82) to WV-7 kerogen (2.13) then decreases in WV-6 kerogen (1.49). The lattice structural parameters in lower and upper Marcellus Formation are similar in individual wells except for the least mature BG-1 well. In the BG-1 well, upper Marcellus has longer aliphatic chain length (Cn'), but lower **C** and SP^2/SP^3 hybridized carbon ratio.

3.2. Control of OM sources and maturity on kerogen structure

Major controls on kerogen structure are sources of OM and thermal maturity [32,39]. If the contribution from marine OM sources is high, the kerogen will have higher alkyl fraction, a longer aliphatic chain length, lesser fractions of oxygen functional groups and bridgehead aromatic carbon as compared to the kerogen composed of more terrestrial OM sources. [32]. On the other hand, increasing maturity will result in a decrease of alkyl fraction, shortening of aliphatic chain

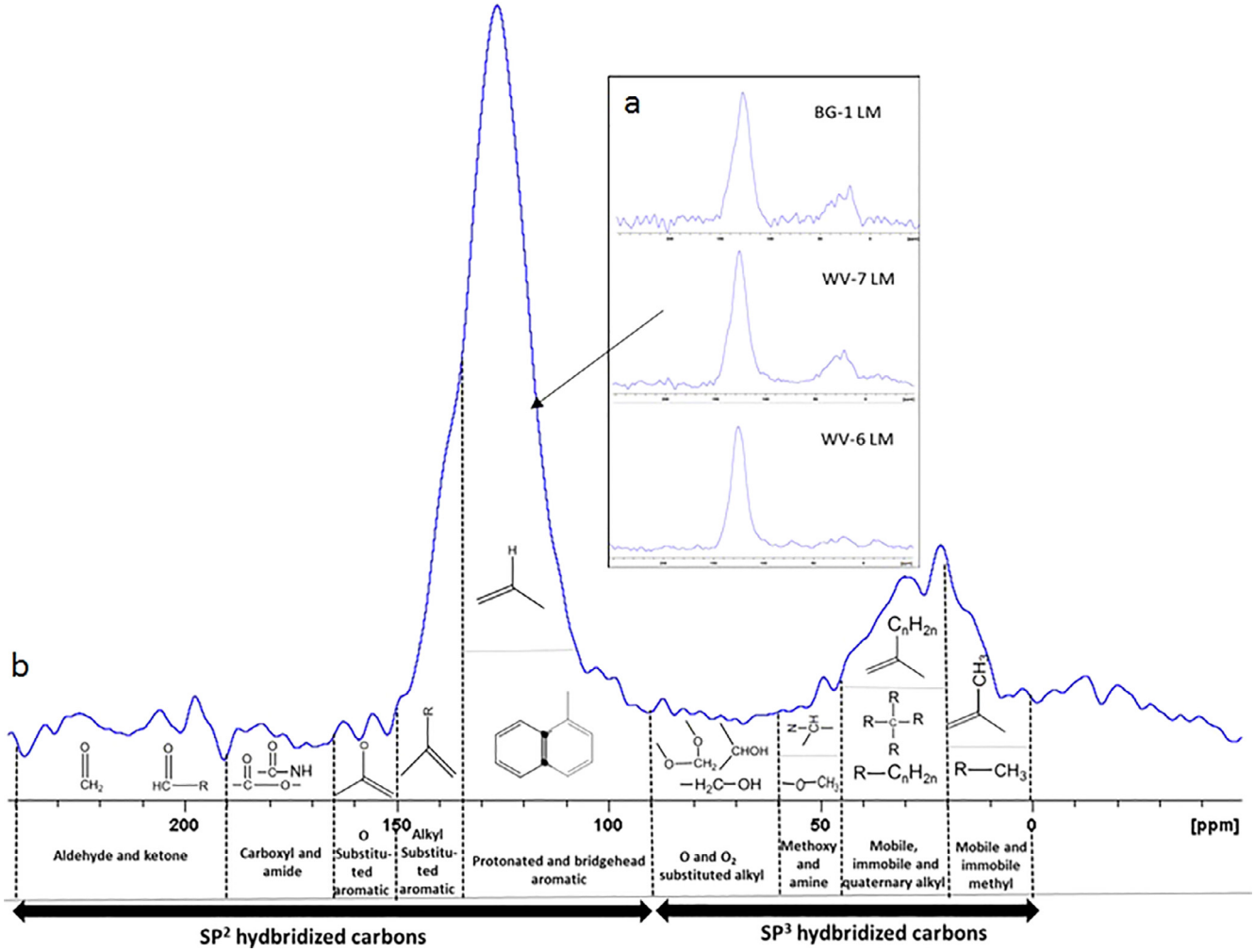

Fig. 2. (a) Multiple CP (cross polarization) ^{13}CNMR spectra of kerogen samples of lower Marcellus Formation from wells BG-1, WV-7, WV-6 LM represents lower Marcellus Shale sample. (b) Spectral range assignment of different functional groups in a spectra, Area of spectra from 0 to 240 ppm was considered to be 100%. Note. DD (dipolar dephasing) spectra are used in regions 0–20, 20–45, 45–60 and 90–135 ppm to determine the percentage of mobile and non-protonated carbon chains.

length and an increase of total aromatic and bridgehead aromatic fraction [39]. The kerogen samples used in this study lie in the oil window (BG-1), wet gas window (WV-7), and dry gas window (WV-6) as supported by production data, geochemical, pyrolysis and biomarker analysis [12,1]. The depositional model proposed by these studies and several other studies [10,11] suggest that the terrestrial sediment influx was from east to west part of the basin. These studies also suggest that sediments in WV-7 well had a lesser influx of terrestrial OM as compared to WV-6 well. Further, it was proposed that upper Marcellus Formation in both WV-6 and WV-7 wells received higher input of terrestrial OM as compared to lower Marcellus Formation. Detailed isotopic and geochemical data is not available for BG-1 well. However,

Table 1
Percentage of different structural parameters/functional groups.

Structural parameters	Chemical Shift (ppm)	BG-1 UM	BG-1 LM	WV-7 UM	WV-7 LM	WV-6 UM	WV-6 LM
Total aliphatic[a]	(0–90)	30.43 ± 1.62	25.49 ± 1.36	25.94 ± 1.38	26.94 ± 1.44	14.82 ± 0.79	13.60 ± 0.73
Alkyl[a]	(0–45)	25.52 ± 2.72	19.92 ± 2.12	21.08 ± 2.25	22.95 ± 2.45	8.18 ± 0.87	9.72 ± 1.04
Mobile methyl[b]	(0–20)	3.46 ± 0.83	3.34 ± 0.80	3.27 ± 0.78	3.23 ± 0.78	0.29 ± 0.07	1.14 ± 0.27
Mobile and quaternary alkyl[b]	(20–45)	5.00 ± 0.96	3.79 ± 0.73	4.08 ± 0.78	3.36 ± 0.65	1.00 ± 0.19	0.85 ± 0.16
Methoxyl and amine[a]	(45–60)	0.92 ± 0.29	2.25 ± 0.72	2.18 ± 0.70	2.14 ± 0.68	1.59 ± 0.51	0.65 ± 0.21
Methoxyl[b]	(45–60)	0.36 ± 0.12	0.30 ± 0.10	0.45 ± 0.14	0.14 ± 0.04	0	0
O and O2 substituted alkyl[a]	(60–90)	3.99 ± 0.64	3.31 ± 0.53	2.68 ± 0.43	1.85 ± 0.30	5.05 ± 0.81	3.23 ± 0.52
Total aromatic[a]	(90–165)	66.61 ± 4.26	70.45 ± 4.51	75.50 ± 4.83	74.60 ± 4.77	84.90 ± 5.43	89.00 ± 5.70
Non-protonated aromatic bridgehead[b]	(90–135)	14.92 ± 1.59	24.97 ± 2.66	29.50 ± 3.15	28.00 ± 2.99	32.90 ± 3.51	36.70 ± 3.91
Protonated aromatic[b]	(90–135)	34.78 ± 3.71	27.70 ± 2.95	32.50 ± 3.47	34.80 ± 3.71	41.20 ± 4.39	43.60 ± 4.65
Alkyl-substituted aromatic[a]	(135–150)	14.86 ± 4.76	16.07 ± 5.14	12.98 ± 4.15	11.86 ± 3.80	10.10 ± 3.23	9.04 ± 2.89
O-substituted aromatic[a]	(150–165)	2.06 ± 0.66	1.72 ± 0.55	0.13 ± 0.04	0.12 ± 0.04	1.00 ± 0.32	0
Carboxyl and amide[a]	(165–190)	4.68 ± 0.90	2.69 ± 0.52	0	0	0.77 ± 0.15	0
Aldehyde and ketone	(190–240)	0*	1.38 ± 0.13	0*	0*	0*	0

NMR method a = cross polarization, b = dipolar-dephasing.
* Values reported as zero but negative values were observed for aldehyde and ketone functional group for some samples (within 2%).

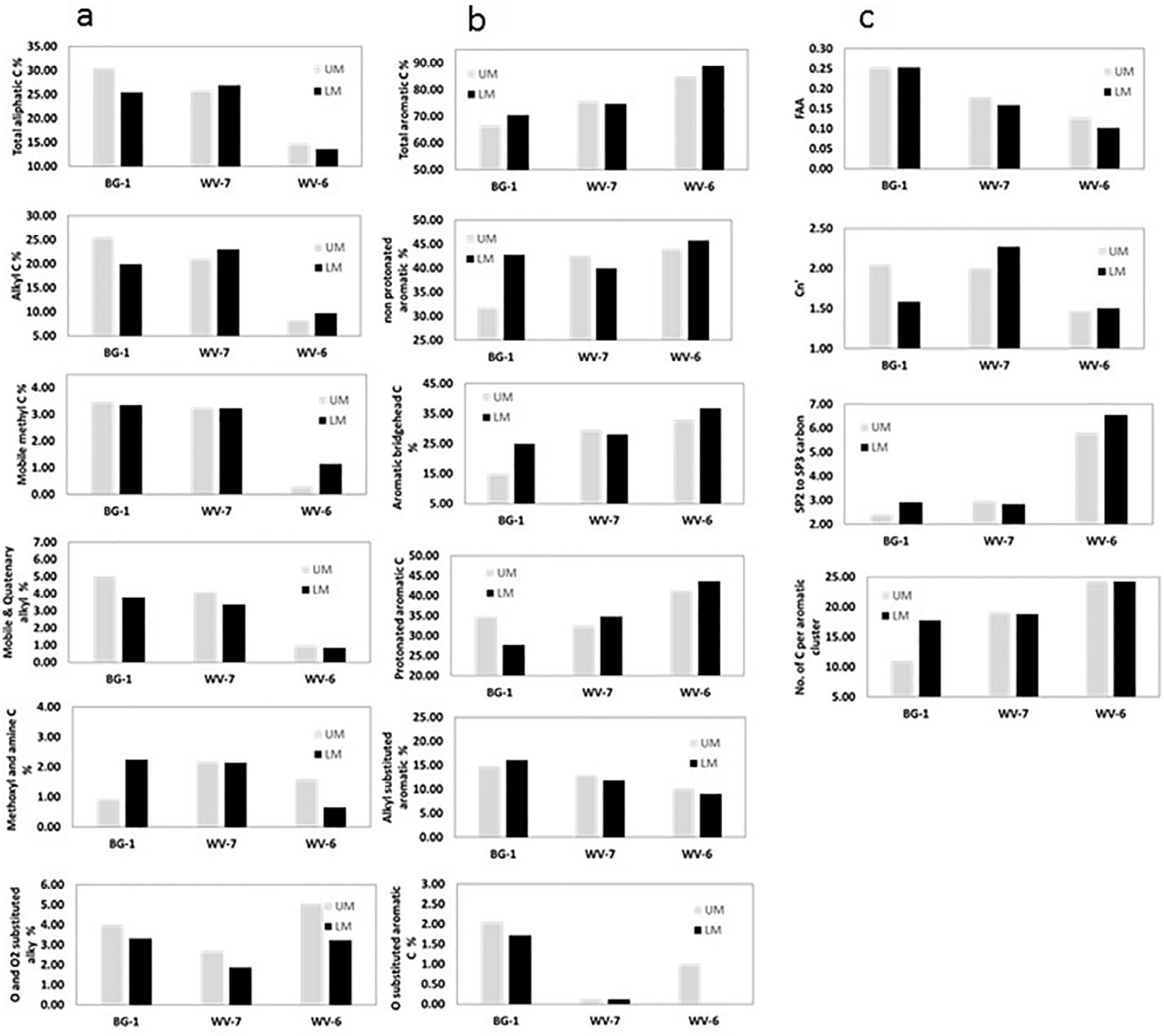

Fig. 3. (a) Percentage of i) Total aliphatic C, ii) alkyl C, iii) mobile methyl, iv) mobile and quaternary alkyl v) methoxy and amine vi) O and O2 substituted alkyl. 3b. Percentage of i) Total aromatic C, ii) non-percentage aromatic C, iii) Protonated aromatic C, iv) Aromatic bridgehead carbon%, v) Alkyl substituted aromatic vi) O substituted, 3c. i) Fraction of aromatic chains with attachments (FAA) ii) Average aliphatic chain length (Cn') iii) SP2 vs SP3 hybridized carbon ration iv) No. of carbon atoms per aromatic cluster (C).

since this well lies in the western part of the basin (Fig. 1), it must have been deposited further away from the terrestrial sediment influx coming from the east.

The kerogen sample from upper Marcellus Formation from BG-1 well (oil window; VRo ~ 08–1.05) shows higher percentage of total aliphatic fraction, alkyl carbon chains(without heteroatoms), protonated aromatic carbon, longer Cn' and lower percentage of aromatic bridgehead carbon, **C,** and SP^2 vs. SP^3 hybridized carbon ratio compared to lower Marcellus Formation (Fig. 3a–c). This suggests that upper Marcellus Formation in the BG-1 well received less terrestrial OM influx compared to the lower Marcellus Formation. This was probably because the sediments in the upper Marcellus Formation in BG-1 well were deposited in the up-dip section of the basin further away from the terrestrial sediment source (as shown by [38]. This suggests that in the oil maturity window (VRo ~ 08–1.05) sources of OM can play a vital role in controlling the kerogen structure. Therefore, in this maturity range, the different structural parameters of kerogen can provide valuable information about changes in sources of OM. In wet gas (WV-7; VRo ~ 1.4) and dry gas (WV-6; VRo ~ 2.5) maturity range, most of the structural parameters such as alkyl carbon percentage (without heteroatoms), total aromatic carbon percent, protonated aromatic percentage, alkyl substituted aromatic, aromatic bridgehead, **C**, FAA, SP^2 to SP^3 hybridized carbon ratio (Fig. 3a–c) were similar for upper and lower Marcellus Formations within the same well. However, isotopic and geochemical evidence from previous studies [12] and [1] indicate that in both these wells lower Marcellus Formation received less influx of terrestrial OM than upper Marcellus. This observation suggests that at higher maturity window (VRo > 1.4), thermal maturity dominantly controls the kerogen structure. A continuous decrease in total aliphatic, alkyl, alkyl substituted aromatic, FAA and a continuous increase in the total aromatic, protonated aromatic carbon, bridgehead carbon, C, SP^2 to SP^3 hybridized carbon ratio from BG-1 to WV-7 to WV-6 kerogen (Fig. 3a–c) also supports that thermal maturity played a major role in structural evolution of mature kerogen. Similar trends for these structural parameters are reported by previous studies [39,25,31]. However, variations in structural parameters such as O and O_2 substituted alkyl

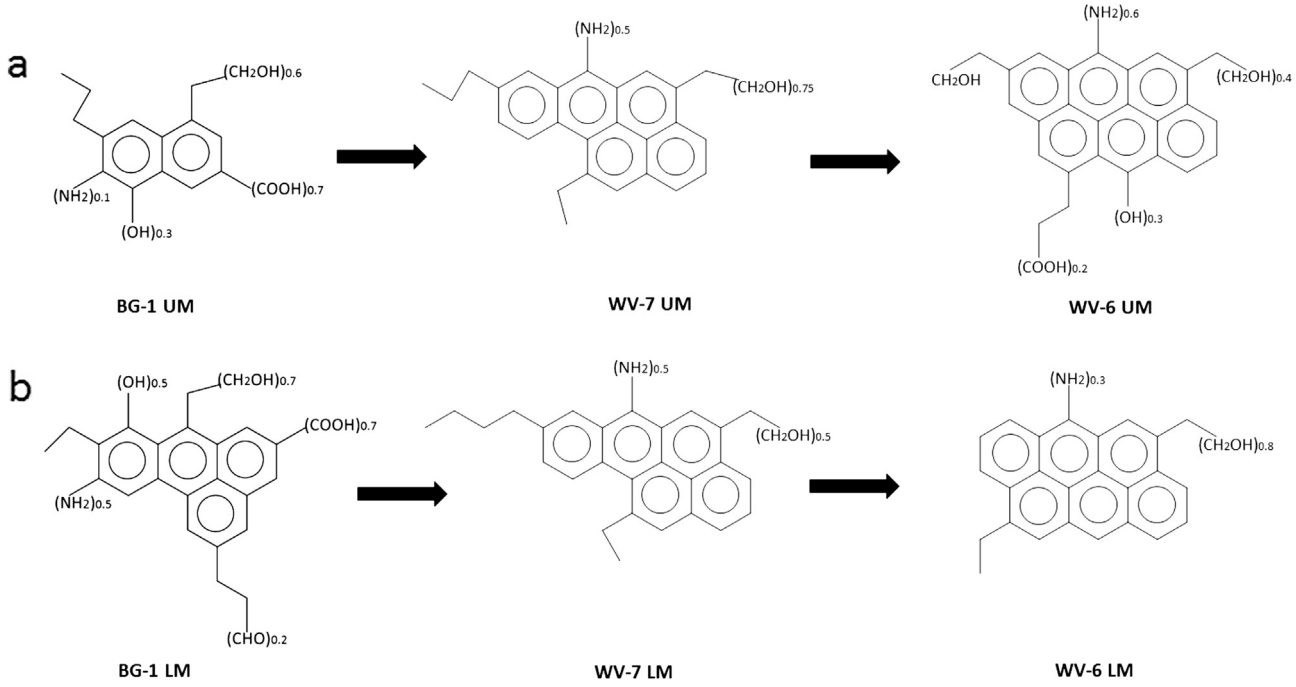

Fig. 4. Schematic representation of transformation of a unit of kerogen cluster from low maturity BG-1 kerogen to higher maturity WV-7 kerogen to further higher maturity WV-6 kerogen. Each unit of kerogen cluster is formed using aliphatic, aromatic and lattice structural parameters (a) upper Marcellus (b) lower Marcellus. Values written in parentheses indicate the fraction of the particular functional group per unit of kerogen cluster. Other isomers of each kerogen unit are possible.

and O- substituted aromatic carbon are contrary to observations made by previous studies [27,39,25,31]. A higher fraction of O and O_2 substituted alkyl groups and O- substituted aromatic carbon for WV-6 kerogen samples is probably because of the higher flux of terrestrial OM received by WV-6 well as proposed by [12]; [1]. These observations suggest that although thermal maturity plays a dominant role in the structural evolution of mature kerogen, the source of OM can still have some effect on a few key structural parameters. This hypothesis is further supported by the fact that variations observed in mobile methyl carbon, amine, and Cn' between the upper and lower Marcellus kerogen from wells WV6 and WV-7, match with the inferences drawn from isotopic and geochemical proxies (Fig. 3a–c). Therefore, we propose that in mature shales (VRo > 1.4), although maturity primarily controls the kerogen structure some inferences can be drawn about sources of OM using selective structural parameters.

3.3. Modeling kerogen evolution, HC generation potential, and maturity

Using the aliphatic, aromatic and lattice structural parameters of kerogen, we propose schematic models for kerogen in oil, wet gas and dry gas windows of Marcellus Shale. (Fig. 4). The schematic representation shows a single cluster of kerogen molecule in upper and lower Marcellus from wells BG-1, WV-7 and WV-6 well (other isomers are also possible). Each cluster is composed of several aromatic rings (based on **C** and bridgehead carbon atoms) and aliphatic attachments. The models show that kerogen structure gets more aromatized with an increase in thermal maturity as seen by previous researchers (for eg. [39,25]. The model also shows that mobile and immobile alkyl, alkyl-substituted aromatic carbons are more prone to thermal degradation compared to carbon chains such as O- substituted alkyl, O_2 substituted alkyl, amine, protonated aromatic carbons, O- substituted aromatic and bridgehead aromatic carbons as they do not show a decline with thermal maturity. It is also observed that lower Marcellus kerogen of BG-1 well is more aromatized and has more aromatic rings as compared to the upper Marcellus Formation indicating higher terrestrial OM input. Samples from the lower and upper Marcellus in WV-7 and WV-6 wells show similar the number of aromatic rings and aromatic fractions. However, previous studies from these wells have proposed that lower Marcellus had more marine OM input compared to upper Marcellus [12,1]. This suggests that at maturity level VRo > 1.4 thermal maturity is the dominant control on kerogen structure as discussed in the previous section.

We also propose that due to lack of understanding of kerogen structure and its cracking mechanism in mature shales, the models proposed to determine their HC potential and thermal maturity might not be accurate. To test this argument, we used regression equations proposed by [31] and [50] to determine the HC potential and thermal maturity of these samples respectively. We compared the hydrocarbon potential values, S2 (hydrocarbons bound to kerogen calculated using pyrolysis analysis) determined from the two equations proposed by [31] with the actual values determined by source rock analyzer. We observed that both regression models highly overestimated the S2 values especially for mature and over-mature WV-7 and WV-6 kerogen samples (Table 4, column 3 and column 4). The primary reason for this overestimation of S2 might be the lower HC potential of O and O_2 substituted aliphatic chains in mature shales. We propose that since [31] used parameters derived from less mature kerogen samples (VRo < 0.8) compared to kerogen samples used in this study, their multiple regression models did not yield reliable results. For our samples, the major changes in structural parameters on maturation was observed in alkyl chains, mainly immobile alkyl chains (Table 1, Fig. 3a). We postulate that from the oil window to dry gas window, the

Table 2
H/C and O/C values of upper and lower Marcellus Formation from WV-6 and WV-7 wells.

Sample	H/C	O/C
BG-1 UM	0.98	0.14
BG-1 LM	0.81	0.12
WV-7 UM	0.84	0.04
WV-7 LM	0.88	0.03
WV-6 UM	0.74	0.08
WV-6 LM	0.71	0.03

Table 3
Average chemical composition of different structural parameters.

	Chemical shift (ppm)	Structural group formula	C	H	O
Mobile and immobile methyl[a]	(0–20)	CH_3	1	3	0
Mobile, immobile and quaternary alkyl[b]	(20–45)	$CH_{1.5}$	1	1.5	0
Methoxy and amine[a]	(45–60)	C $H_{1.5}$ $O_{0.5}$, $CNH_{1.5}$	1	1.5	0.5
O-substituted alkyl and O2 substituted alkyl[a]	(60–90)	$CH_{2.5}O$	1	2.5	1
Protonated aromatic[b]	Total aromatic (90–135)-non protonated 90–135)	CH	1	1	0
Bridgehead aromatic carbon[b]	(90–135)	C	1	0	0
Alkyl-substituted aromatic[a]	(135–145)	C	1	0	0
O-substituted aromatic[a]	(145–165)	$COH_{0.5}$	1	0.5	1
Carboxyl and amide[a]	(165–190)	$CO_{1.75}H_{0.5}$, CONH	1	0.5	1.75
Aldehyde and ketone[a]	(190–220)	$COH_{0.5}$	1	0.5	1

NMR method a = cross polarization or direct polarization, b = dipolar-dephasing.

Table 4
True and calculated values of hydrocarbon potential (S2) and Vitrinite reflectance (VRo).

Sample	True S2[a]	S2[b]	S2[c]	True VRo[a,d]	VRo[e]
BG-1 UM	5.11	12.51	10.56	1	1.06
BG-1 LM	15.84	12.32	27.69	0.81	0.71
WV 7 UM	1.41	10.77	26.35	1.4[a]	0.56
WV-7 LM	10.67	12.12	40.35	1.4[a]	0.47
WV-6 UM	0.02	7.60	14.61	> 2.5[d]	1.42
WV-6 LM	0.47	1.85	40.40	> 2.5[d]	1.80

a = taken from [1].
b = calculated using Eq. 1 of [31].
c = calculated using Eq. 2 of [31].
d = taken from [53].
e = calculated using Eq. 12 of [50].

immobile alkyl chains are the main contributors of HC generation by kerogen cracking.

[50] suggested an equation for determining thermal maturity using kerogen structural parameters. However, the equations proposed underestimates the VRo values for the kerogen samples of WV-7 and WV-6 wells (Table 4, column 6). Similar observations of overestimation of S2 parameter and underestimation of thermal maturity using previously built models can be observed for another over mature well MIP-3H with VRo ~ 2.9 [2]. Therefore we propose for precise estimation of HC potential and thermal maturity in mature shales we need to construct new kerogen models that are based on structural parameters derived from samples from mature shales.

3.4. Evaluation of kerogen type

The traditional van Krevelen diagram generated from SRA analysis using the hydrogen index (HI) and oxygen index (OI) cannot be used to determine kerogen type in the mature shales used in this study. This is due to low HI and OI in all samples (as shown in Fig. 5a, [1]. However, molecular level characterization of kerogen using solid-state methods gives us the opportunity to determine the accurate chemical composition of kerogen. Since each structural parameter has a particular composition (for example CH_3 for methyl group), an average chemical composition to each structural parameter of kerogen can be assigned (as shown in Table 3). Also, since the fraction of each structural parameter is known, the relative amount of H, C, and O of each structural parameter of kerogen can be determined by multiplying the fraction of each structural parameter with the number of H/C/O present in the molecular formula of the functional group as shown in Table 2 (e.g., for methyl group CH_3, 1 carbon atom a 3 hydrogen atoms will be considered). By dividing the relative total fraction of H, C, and O the H/C and O/C ratios can be determined as shown in Table 2. This method is known as direct assignment (DA) method as proposed by Hockaday et al. [19]. The values of H/C and O/C calculated from DA method suggests that shale from both upper and lower Marcellus Formation of BG-1, WV-7, and WV-6 wells belong to type II to type III kerogen (Fig. 5b). Similar interpretations were made using the biomarker analysis for the same set of WV-6 and WV-7 samples by [2]. This observation suggests that H, C, and O amounts derived from structural parameters of kerogen can provide valuable information about OM sources/type in mature shale systems where traditional methods like SRA fail.

4. Conclusions

Data generated from direct kerogen analysis suggests that samples from most mature Marcellus Shale well lying in a dry gas window (WV-6) had the highest fraction of aromatic carbon followed by samples from the wet gas window (WV-7) and oil window (BG-1). This is in agreement with the previously published studies on the structural evolution of kerogen. Our results also indicate that most of the aliphatic and aromatic structural parameters of kerogen in upper and lower Marcellus Formation are similar in wells WV-6 and WV-7 (VRo > 1). However, previous studies suggest sediments in these wells were deposited in different part of the basin and received different terrestrial and marine OM influx. This suggests that at high maturity levels thermal maturity is the dominant control on kerogen structure. However, OM sources can still be discerned using certain kerogen lattice structural parameters such as O and O2 substituted alkyl, O- substituted aromatic carbon, mobile methyl carbon, and Cn'. In contrast, at lower maturity (VRo < 1), OM sources play a key role in controlling the kerogen structure.

Our results indicate that carbon chains such as mobile and immobile alkyl, alkyl-substituted aromatic carbons are more prone to thermal degradation and therefore might have higher hydrocarbon generating potential as compared to functional groups such O- substituted alkyl, O2 substituted alkyl, amine, protonated aromatic carbons, O- substituted aromatic and bridgehead aromatic carbons. We also propose that previous models routinely used for determining hydrocarbon potential and thermal maturity of shales cannot be used for mature shale systems with VRo > 1 like the Marcellus. We are currently in the process of acquiring shale samples across the entire maturity series to conduct additional kerogen studies to develop precise HC generation and maturity models for mature shale systems.

Acknowledgments

The research was funded by Department of Energy's National Energy Technology Laboratory (DE# FE0024297; DE# FE0004000) and National Science Foundation (NSF DEB-1342732) grants to S. Sharma. The authors thank Dr. Jingdong Mao and Wenying Chu from Old Dominion University, VA for ^{13}C NMR analysis and Dr. Ajay Warrier from the WVU IsoBioGem Lab for help with sample preparation. West Virginia Geological and Economic Survey and Southwestern Energy are acknowledged for providing samples for the study. We also

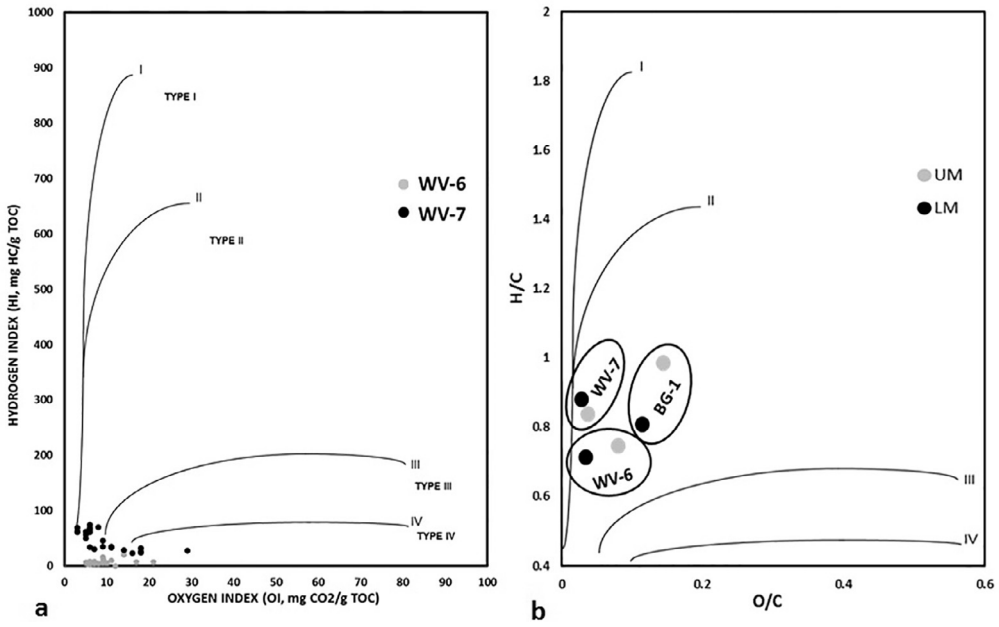

Fig. 5. (a) van Krevelen diagram showing type of kerogen samples from upper and lower Marcellus Formation of WV-6 and WV-7 wells using pyrolysis (taken from [1] (b) van Krevelen diagram showing mixed type II-type III kerogen for 6 kerogen samples from upper and lower Marcellus Formation of BG-1, WV-7 and WV-6 using DA method.

thank the reviewers for their insightful comments and suggestions.

Appendix A. Supplementary data

Supplementary data associated with this article can be found, in the online version, at http://dx.doi.org/10.1016/j.fuel.2018.04.053.

References

[1] Agrawal V, Sharma S. Testing utility of organogeochemical proxies to assess sources of organic matter, paleoredox conditions and thermal maturity in mature Marcellus Shale. Front Energy Res 2018. (in press).

[2] Agrawal V, Sharma S. Direct kerogen characterization of Marcellus Shale collected from Marcellus Shale Energy and Environment Laboratory. Morgantown, WV: Eastern AAPG; 2017.

[3] Arfaoui A, Montacer M, Kamoun F, Rigane A. Comparative study between Rock-Eval pyrolysis and biomarkers parameters: a case study of Ypresian source rocks in central-northern Tunisia. Mar Pet Geol 2007;24(10):566–78. http://dx.doi.org/10.1016/j.marpetgeo.2007.05.002.

[4] Baldock JA, Masiello CA, Gélinas Y, Hedges JI. Cycling and composition of organic matter in terrestrial and marine ecosystems. Mar Chem 2004;92(1):39–64. http://dx.doi.org/10.1016/j.marchem.2004.06.016.

[5] Behar F, Vandenbroucke M. Chemical modelling of kerogens. Org Geochem 1987;11(1):15–24. http://dx.doi.org/10.1016/0146-6380(87)90047-7.

[6] Behar F, Vandenbroucke M, Tang Y, Marquis F, Espitalie J. Thermal cracking of kerogen in open and closed systems: determination of kinetic parameters and stoichiometric coefficients for oil and gas generation. Org Geochem 1997;26(5):321–39. http://dx.doi.org/10.1016/S0146-6380(97)00014-4.

[7] Boucher RJ, Standen G, Patience RL, Eglinton G. Molecular characterisation of kerogen from the Kimmeridge clay formation by mild selective chemical degradation and solid state 13C-NMR. Org Geochem 1990;16(4):951–8. http://dx.doi.org/10.1016/0146-6380(90)90131-I.

[8] Cao X, Chappell MA, Schimmelmann A, Mastalerz M, Li Y, Hu W, et al. Chemical structure changes in kerogen from bituminous coal in response to dike intrusions as investigated by advanced solid-state 13C NMR spectroscopy. Int J Coal Geol 2013;108(Supplement C):53–64. http://dx.doi.org/10.1016/j.coal.2012.05.002.

[9] Cao X, Yang J, Mao J. Characterization of kerogen using solid-state nuclear magnetic resonance spectroscopy: a review. Int J Coal Geol 2013;108(Supplement C):83–90. http://dx.doi.org/10.1016/j.coal.2011.12.001.

[10] Chen R, Sharma S. Role of alternating redox conditions in the formation of organic-rich interval in the Middle Devonian Marcellus Shale, Appalachian Basin, USA. Palaeogeogr Palaeoclimatol Palaeoecol 2016;446(Supplement C):85–97. http://dx.doi.org/10.1016/j.palaeo.2016.01.016.

[11] Chen R, Sharma S. Linking the Acadian Orogeny with organic-rich black shale deposition: evidence from the Marcellus. Shale Mar Petroleum Geol 2017;79(Supplement C):149–58. http://dx.doi.org/10.1016/j.marpetgeo.2016.11.005.

[12] Chen R, Sharma S, Bank T, Soeder D, Eastman H. Comparison of isotopic and geochemical characteristics of sediments from a gas- and liquids-prone wells in Marcellus Shale from Appalachian Basin, West Virginia. Appl Geochem 2015;60(Supplement C):59–71. http://dx.doi.org/10.1016/j.apgeochem.2015.01.001.

[13] Dennis LW, Maciel GE, Hatcher PG, Simoneit BRT. 13C Nuclear magnetic resonance studies of kerogen from Cretaceous black shales thermally altered by basaltic intrusions and laboratory simulations. Geochim Cosmochim Acta 1982;46(6):901–7. http://dx.doi.org/10.1016/0016-7037(82)90046-1.

[14] Durand B. 1980. Kerogen: Insoluble Organic Matter from Sedimentary Rocks. Editions TECHNIP.

[15] Elie M, Faure P, Michels R, Landais P, Griffault L. Natural and laboratory oxidation of low-organic-carbon-content sediments: comparison of chemical changes in hydrocarbons. Energy Fuels 2000;14(4):854–61. http://dx.doi.org/10.1021/ef9902146.

[16] Espitalie J, Deroo G, Marquis F. Rock-Eval pyrolysis and its applications. Rev Inst Fr Pet 1985;40:563–79.

[17] Freund H, Walters CC, Kelemen SR, Siskin M, Gorbaty ML, Curry DJ, et al. Predicting oil and gas compositional yields via chemical structure–chemical yield modeling (CS-CYM): Part 1 – Concepts and implementation. Org Geochem 2007;38(2):288–305. http://dx.doi.org/10.1016/j.orggeochem.2006.09.009.

[18] Hedges JI. Polymerization of humic substances in natural environments. Frimmel FH, Christman RF, editors. Humic Substances and Their Role in the Environment John Wiley and Sons Ltd.; 1988. p. 45–58.

[19] Hockaday WC, Masiello CA, Randerson JT, Smernik RJ, Baldock JA, Chadwick OA, et al. Measurement of soil carbon oxidation state and oxidative ratio by 13C nuclear magnetic resonance. J Geophys Res Biogeosci 2009;114(G2):G02014. http://dx.doi.org/10.1029/2008JG000803.

[20] Horsfield B. Practical criteria for classifying kerogens: some observations from pyrolysis-gas chromatography. Geochim Cosmochim Acta 1989;53(4):891–901. http://dx.doi.org/10.1016/0016-7037(89)90033-1.

[21] Huc AY, Durand B. 1974. Etudes des acides humiques et de l'humine de sediments recents consideres comme precurseurs des kerogenes. In: Advances in Organic Geochemistry, 1973. Technip, Paris, p. 53.

[22] Ibrahimov RA, Bissada (Adry) KK. Comparative analysis and geological significance of kerogen isolated using open-system (palynological) versus chemically and volumetrically conservative closed-system methods. Org Geochem 2010;41(8):800–11. http://dx.doi.org/10.1016/j.orggeochem.2010.05.006.

[23] Johnson RL, Schmidt-Rohr K. Quantitative solid-state 13C NMR with signal enhancement by multiple cross polarization. J Magn Reson 2014;239(Supplement C):44–9. http://dx.doi.org/10.1016/j.jmr.2013.11.009.

[24] Shen J-Chin, Huang W-Liang. Biomarker distributions as maturity indicators in coals, coaly shales, and shales from taiwan. Terrestrial Atmos Oceanic Sci 2007;18(4):739–55. http://dx.doi.org/10.3319/TAO.2007.18.4.739(TT).

[25] Kelemen SR, Afeworki M, Gorbaty ML, Sansone M, Kwiatek PJ, Walters CC, et al. Direct Characterization of Kerogen by X-ray and Solid-State 13C Nuclear Magnetic Resonance Methods. Energy Fuels 2007;21(3):1548–61. http://dx.doi.org/10.1021/ef060321h.

[26] Kroon J. 2011. Biomarkers in the Lower Huron Shale (Upper Devonain) as indicators of organic matter source, depositional environment, and thermal maturity. All Theses. Retrieved from https://tigerprints.clemson.edu/all_theses/1166

[27] Kuangzong Q, Deyu C, Zhanguang L. A new method to estimate the oil and gas potentials of coals and kerogens by solid state 13C NMR spectroscopy. Org Geochem 1991;17(6):865–72. http://dx.doi.org/10.1016/0146-6380(91)90026-G.

[28] Lewan MD, Ruble TE. Comparison of petroleum generation kinetics by isothermal hydrous and nonisothermal open-system pyrolysis. Org Geochem 2002;33(12):1457–75. http://dx.doi.org/10.1016/S0146-6380(02)00182-1.

[29] Lille Ü, Heinmaa I, Pehk T. Molecular model of Estonian kukersite kerogen

evaluated by 13C MAS NMR spectra☆. Fuel 2003;82(7):799–804. http://dx.doi.org/10.1016/S0016-2361(02)00358-7.
[30] Longbottom TL, Hockaday WC, Boling KS, Dworkin SI. Effect of ocean oxidation on the chemical structure of marine kerogen. Organic Geochem 2017;106(Supplement C):1–12. http://dx.doi.org/10.1016/j.orggeochem.2017.01.002.
[31] Longbottom TL, Hockaday WC, Boling KS, Li G, Letourmy Y, Dong H, et al. Organic structural properties of kerogen as predictors of source rock type and hydrocarbon potential. Fuel 2016;184(Supplement C):792–8. http://dx.doi.org/10.1016/j.fuel.2016.07.066.
[32] Mann Al, Patience Rl, Poplett IJF. Determination of molecular structure of kerogens using 13C NMR spectroscopy: I. The effects of variation in kerogen type. Geochimica et Cosmochimica Acta 1991;55(8):2259–68. http://dx.doi.org/10.1016/0016-7037(91)90102-B.
[33] Mao J, Fang X, Lan Y, Schimmelmann A, Mastalerz M, Xu L, et al. Chemical and nanometer-scale structure of kerogen and its change during thermal maturation investigated by advanced solid-state 13C NMR spectroscopy. Geochim Cosmochim Acta 2010;74(7):2110–27. http://dx.doi.org/10.1016/j.gca.2009.12.029.
[34] Mao J-D, Schmidt-Rohr K. Recoupled long-range C-H dipolar dephasing in solid-state NMR, and its use for spectral selection of fused aromatic rings. J Magn Reson 2003;162(1):217–27. http://dx.doi.org/10.1016/S1090-7807(03)00012-0.
[35] Mao J-D, Schmidt-Rohr K. Accurate quantification of aromaticity and non-protonated aromatic carbon fraction in natural organic matter by 13C solid-state nuclear magnetic resonance. Environ Sci Technol 2004;38(9):2680–4. http://dx.doi.org/10.1021/es034770x.
[36] Mao J-D, Tremblay L, Gagné J-P, Kohl S, Rice J, Schmidt-Rohr K. Humic acids from particulate organic matter in the Saguenay Fjord and the St. Lawrence Estuary investigated by advanced solid-state NMR. Geochim Cosmochim Acta 2007;71(22):5483–99. http://dx.doi.org/10.1016/j.gca.2007.09.022.
[37] Martínez M, Escobar M. Effect of coal weathering on some geochemical parameters. Org Geochem 1995;23(3):253–61. http://dx.doi.org/10.1016/0146-6380(94)00115-H.
[38] Parrish CB. Insights into the Appalachian Basin Middle Devonian Depositional System from U-Pb Zircon Geochronology of Volcanic Ashes in the Marcellus Shale and Onondaga Limestone. M.S: West Virginia University; 2013.
[39] Patience RL, Mann AL, Poplett IJF. Determination of molecular structure of kerogens using 13C NMR spectroscopy: II. The effects of thermal maturation on kerogens from marine sediments. Geochim Cosmochim Acta 1992;56(7):2725–42. http://dx.doi.org/10.1016/0016-7037(92)90356-N.
[40] Peters KE, Walters CC, Moldowan JM. The Biomarker Guide. Cambridge University Press; 2005.
[41] Petersen HI, Rosenberg P, Nytoft HP. Oxygen groups in coals and alginite-rich kerogen revisited. Int J Coal Geol 2008;74(2):93–113. http://dx.doi.org/10.1016/j.coal.2007.11.007.
[42] Siskin M, Scouten CG, Rose KD, Aczel T, Colgrove SG, Pabst RE. 1995. Detailed Structural Characterization of the Organic Material in Rundle Ramsay Crossing and Green River Oil Shales. In: Composition, Geochemistry and Conversion of Oil Shales (pp. 143–158). Springer, Dordrecht. doi: 10.1007/978-94-011-0317-6_9.
[43] Smernik RJ, Oades JM. Solid-state 13C-NMR dipolar dephasing experiments for quantifying protonated and non-protonated carbon in soil organic matter and model systems. Eur J Soil Sci 2001;52(1):103–20. http://dx.doi.org/10.1046/j.1365-2389.2001.00364.x.
[44] Solum MS, Pugmire RJ, Grant DM. Carbon-13 solid-state NMR of Argonne-premium coals. Energy Fuels 1989;3(2):187–93. http://dx.doi.org/10.1021/ef00014a012.
[45] Tissot BP, Welte DH. Petroleum formation and occurrence. Springer-Verlag; 1984.
[46] Tong J, Han X, Wang S, Jiang X. Evaluation of structural characteristics of huadian oil shale kerogen using direct techniques (Solid-State 13C NMR, XPS, FT-IR, and XRD). Energy Fuels 2011;25(9):4006–13. http://dx.doi.org/10.1021/ef200738p.
[47] Vandenbroucke M. Kerogen: from types to models of chemical structure. Oil Gas Sci Technol 2003;58(2):243–69. http://dx.doi.org/10.2516/ogst:2003016.
[48] Vandenbroucke M, Largeau C. Kerogen origin, evolution and structure. Org Geochem 2007;38(5):719–833. http://dx.doi.org/10.1016/j.orggeochem.2007.01.001.
[49] Walters CC, Freund H, Kelemen SR, Peczak P, Curry DJ. Predicting oil and gas compositional yields via chemical structure–chemical yield modeling (CS–CYM): part 2 – application under laboratory and geologic conditions. Org Geochem 2007;38(2):306–22. http://dx.doi.org/10.1016/j.orggeochem.2006.09.010.
[50] Wei Z, Gao X, Zhang D, Da J. Assessment of thermal evolution of kerogen geopolymers with their structural parameters measured by solid-state 13c nmr spectroscopy. Energy Fuels 2005;19(1):240–50. http://dx.doi.org/10.1021/ef0498566.
[51] Werner-Zwanziger U, Lis G, Mastalerz M, Schimmelmann A. Thermal maturity of type II kerogen from the New Albany Shale assessed by 13C CP/MAS NMR. Solid State Nucl Magn Reson 2005;27(1):140–8. http://dx.doi.org/10.1016/j.ssnmr.2004.08.001.
[52] Witte EG, Schenk HJ, Müller PJ, Schwochau K. Structural modifications of kerogen during natural evolution as derived from 13C CP/MAS NMR, IR spectroscopy and Rock-Eval pyrolysis of Toarcian shales. Org Geochem 1988;13(4):1039–44. http://dx.doi.org/10.1016/0146-6380(88)90286-0.
[53] Zagorski WA, Wrightstone GR, Bowman DC. The Appalachian Basin Marcellus gas play: its history of development, geologic controls on production, and future potential as a world-class reservoir. Am Assoc Pet Geol Mem 2012;97:172–200.
[54] East, J.A., Swezey, C.S., Repetski, J.E., Hayba, D.O., 2012. Thermal Maturity Map of Devonian Shale in the Illinois, Michigan, and Appalachian Basins of North America. U.S. Geological Survey, Scientific Investigations Map 3214, 1 Sheet.